Supplementary Materials for

27-Hydroxycholesterol Links Hypercholesterolemia and Breast Cancer Pathophysiology

Erik R. Nelson, Suzanne E. Wardell, Jeff S. Jasper, Sunghee Park, Sunil Suchindran, Matthew K. Howe, Nicole J. Carver, Ruchita V. Pillai, Patrick M. Sullivan, Varun Sondhi, Michihisa Umetani, Joseph Geradts and Donald P. McDonnell.

Correspondence to: donald.mcdonnell@duke.edu

This PDF file includes:

Materials and Methods

All studies involving the use of animals were conducted after prior approval by the Duke institutional animal care and use committee (IACUC).

In vitro Assays:

MCF7, T47D, BT483 and BT474 cells were maintained in DMEM/F12, DMEM, RPMI 1640 or RPMI 1640, respectively, supplemented with 8% fetal bovine serum, nonessential amino acids and sodium pyruvate. For experiments, cells were plated in the same media lacking phenol red and supplemented with 8% charcoal-stripped fetal bovine serum. Expression profiling of 27HC in MCF7 cells, uploaded to GEO as GSE46924, was part of a larger study (GSE35428) that has been previously published (*28*). All cells were treated with 27HC at 1μM for 24h. Microarray analysis was performed in R/Bioconductor using the Affy package. Raw data was background corrected with RMA, Log2 transformed, and summarized by medianpolish. Differentially expressed genes were called using the LIMMA package and p-values were corrected for multiple testing with the Benjamini-Hochberg procedure. The expression heatmap was generated in R and ontology enrichment was performed in HOMER. RNA isolation quantitative real time PCR (QPCR) and proliferation assays were performed as previously described (*15*).

MCF7 Xenografts:

Athymic nude mice were ovariectomized and either implanted with a timed-release E2 pellet (0.72 mg E2/60d), placebo (no hormone) pellet, or treated with 27HC (40mg/kg/day). Seven days post-surgery, MCF7 tumors were orthotopically grafted into the axial mammary fat pad. When E2 tumors reached a size of $0.2cm^3$, this group was randomized into vehicle treated or ICI 182,780 treated (weekly injection of 5mg/mouse). After 40d, the 27HC treated mice were randomized into either continued 27HC, no hormone withdrawal or 27HC + ICI 182,780.

Tamoxifen resistant MCF7 Xenograft:

Tamoxifen resistant tumors were previously established by serial transfer in mice treated with tamoxifen (*18*). Experimental mice were ovariectomized and either implanted with a timed-release E2 pellet (0.72 mg E2/60d), timed-release tamoxifen pellet (5 mg/60d) or treated with either 27HC (40mg/kg/day) or vehicle (no hormone). Two days post-surgery, tumors (~$0.8\text{-}1cm^3$) grown in tamoxifen treated donor mice were removed, cut into $2mm^3$ cubes and inserted orthotopically into the axial mammary fat pad of experimental mice.

PyMT Tumor Studies:

Genetic Elevation of 27HC: $CYP7B1^{+/+}$ and $CYP7B1^{-/-}$ mice are maintained on a mixed 129/C57BL/6 background. $CYP7B1^{-/-}$ were bred with MMTV-PyMT+ mice on an FVB background. Resulting heterozygous (CYP7B1+/-;PyMT+) progeny were crossed with either $CYP7B1^{+/+}$ or $CYP7B1^{-/-}$ mice to create homozygous wildtype or knockout mice expressing PyMT. These mice were again crossed with their respective CYP7B1 line to create breeding PyMT+ males of the appropriate genotype. The males of this generation were bred with their respective CYP7B1 line to generate the PyMT+ females used in experiments. Thus, we established $CYP7B1^{+/+}$; PyMT+ and $CYP7B1^{-/-}$;PyMT+ females.

At ~5 weeks of age, mice were ovariectomized. Mice were monitored for first palpable tumors, the growth of which was then recorded through time.

Pharmacologic Elevation of 27HC: MMTV-PyMT+ mice on an FVB background were obtained from Jackson Labs and bred in house. At ~5 weeks of age mice were ovariectomized. Mice were monitored for first palpable tumors. At detection, daily treatment with placebo, 27HC (40mg/kg), GW3965 (30mg/kg) or E2 (10μg/kg). The effectiveness of this strategy as a means to elevate circulating 27HC was demonstrated previously by our laboratory (*13*). After 28 days of treatment, serum 27HC concentrations were increased by approximately 40 fold in 27HC treated mice. Resulting plasma concentrations after 28 days of treatment were approximately 4.5μM. This is similar to concentrations found in patients with mutations in the CYP7B1 gene, although higher levels are apparent in atherosclerotic lesions, (in the millimolar range). In this study, plasma levels of 27HC were 40-50 fold higher in PyMT mice treated with 27HC compared to placebo. Mice were euthanized when their collective tumor burden reached $2cm^3$.

High Cholesterol Diet Studies: MMTV-PyMT+ mice were bred with either wildtype or $CYP27A1^{-/-}$ mice on a C57BL/6 background using a similar strategy to the CYP7B1 mice described above. Thus we established $CYP27A1^{+/+}$; PyMT+ and $CYP27A1^{-/-}$;PyMT+ females. At wean (21 days) mice were placed on either a control diet (TestDiet 5001) or a high cholesterol diet (2% cholesterol, 0.5% sodium cholate), *ad libitum*. The addition of cholate abrogates the bile acid synthesis deficit and thus poor cholesterol absorption in $CYP27A1^{-/-}$ mice. At ~5 weeks of age mice were ovariectomized. Mice were monitored for first palpable tumors, the growth of which was then recorded through time.

E0771 Tumor Studies:

C57BL/6 mice were purchased from Charles River Laboratories Inc. and ovariectomized. E0771 cells were cultured in RPMI plus non-essential amino acids, sodium pyruvate and 8% FBS. 10-days post-ovariectomy, E0771 were orthotopically grafted into the axial mammary fat pad. Treatments were administered daily by subcutaneous injection. Doses of indicated ligand were the same as for the PyMT tumor growth studies.

High fat diet studies in human apoE3 mice:

Human *apoE3* transgenic replacement mice were generated previously (*27*). The control (CD) and high fat diets (HFD) were purchased from TestDiet (5TJS and 5TJN respectively). To evaluate the effect of a high fat diet male *apoE3* mice were placed on a CD or HFD for 8 weeks prior to blood draw and/or tumor graft. For tumor studies, females were ovariectomized between 6-8 weeks of age and placed on their respective diets for 8 weeks. At this point treatment with indicated ligands was initiated and E0771 cells orthotopically grafted into the mammary fat pad. The CYP27A1 inhibitor GW27329TX was administered daily (100mg/kg) subcutaneously. Atorvastatin was administered by daily oral gavage (40mg/kg).

Relapse Free Survival analysis for CYP27A1 and CYP7B1 mRNA:

An integrative database comprising 4022 patients from 22 publicly available datasets was assembled for querying. The raw data was downloaded from GEO, normalized with RMA and batch corrected using the COMBAT algorithm within R. Clinical data was also aggregated from GEO and duplicate patient samples were filtered out. Each tumor was then classified into tumor subtypes using the PAM50, MOD1, and MOD2 gene modules in Genefu (*29, 30*). Gene expression was split by the median into Low and High classifications. Reported p-values were calculated using the log-rank method. Datasets used: GSE11121, GSE12093, GSE12276, GSE1456, GSE16391, GSE16446, GSE19615, GSE22035, GSE22093, GSE23720, GSE26639, GSE3494, GSE5327, GSE6532, GSE7390, GSE9195, GSE17705, GSE2034, GSE20685, GSE21653, GSE4922, GSE6532.

Human Tissues:

We used tissue microarrays that included duplicate 1 mm cores of formalin fixed, paraffin embedded primary human breast carcinomas from a group of 59 interpretable tumors from Vienna, Austria (*31*). For all tumors, grade and ER/PR/HER2 biomarker data were available.

CYP27A1 IHC Analysis:

TMA sections were deparaffinized, treated with sub-boiling antigen retrieval buffer (citrate, pH 6) for 20 minutes, and then reacted with an anti-CYP27A1 rabbit monoclonal antibody (ab126785 from Abcam) at 1:500 for 2 hours. The detection reaction utilized the rabbit Envision kit from Dako. Diaminobenzidine (DAB) was used as chromogen, with hematoxylin as counterstain. The IHC experiments were performed on an automated immunostainer (Intellipath from Biocare). Paraffin-embedded cell blocks of HEPG2 cells and normal human liver tissue served as external positive controls. Positive cells showed granular cytoplasmic reactivity. Positive cells showed granular cytoplasmic reactivity. A blocking peptide (ab139504) was able to ablate the signal. All analysis including cell type identification and staining intensity was performed by a board certified pathologist. Macrophages were identified by morphology. Staining intensity in tumor cells was scored as 0 (absent), 0.5 (borderline), 1 (weak), 2 (moderate) or 3 (strong). For statistical analysis, the tumors were categorized as weak (0, 0.5, 1), and overexpressed (2,3). Ordinal logistic regression was used for binary outcomes and proportional odds regression was used for Grade. Score was modeled as a binary predictor with levels weak and overexpressed. For outcomes with low cell counts a Fisher's exact test of association was used. Analyses were conducted in SAS version 9.3 (SAS Institute, Cary, NC) and the R environment for statistical computing (*32*).

MMTV-PyMT Lung Metastasis:

For the MMTV-PyMT models, mice were euthanized when their collective tumor size reached $2cm^3$. Mice were randomized into their lungs being extracted and frozen, or inflated with 10% formalin. RNA was extracted from frozen lungs and probed for PyMT transcript by QPCR. Formalin inflated lungs were fixed overnight and then preserved in 70% ethanol. They were then dehydrated, paraffin embedded, sectioned and stained with H&E.

Lung Colonization:

IRFP expressing plasmid (Addgene 31857) was subcloned into pENTR2B (Invitrogen) to generate the Gateway®-compatible entry vector, pENTR2B-iRFP construct. To generate a lentivirus expressing IRFP, pENTR2B-IRFP was recombined with the destination vector, pLenti-CMV/TO Neo DEST (Addgene 17292) using LR reaction. Stable IRFP expressing Met1 cells were established by flow cytometry. Met1 cells were stably expressing IRFP were pretreated in culture with either vehicle, 27HC or GW3965 for 72hrs. They were then injected (iv) into syngeneic recipient mice. 28 days later, mice were sacrificed, lungs were canulated, re-inflated with PBS and imaged with an IVIS-Kenetic machine (Caliper Life Sciences).

Statistics:

Values were assessed for normality and where appropriate either ln-transformed or a non-parametric test was selected. Figure 1B,F, Figure 2C,D: 2-way ANOVA followed by Bonferroni's post-hoc t-test. Figure 1C,D,E, Figure 2A,B, Figure S6, S13C,D: Kaplan-Meier curves compared to each other using log rank test. Figure 3B,D, Figures S10B, S11A,B, S12A and S13A,B: unpaired two tailed student's t-test compared between two groups. Figures S2, S3, S5, S8, S10A, S11C, S12B and S14: 1-way ANOVA followed by Student Newman-Keuls multiple comparison post-hoc test, or Kruskal-Wallis followed by Dunn's multiple comparison test. Figure S12: linear regression was performed and slope compared to null hypothesis of 0. Graphpad Prism was used for analysis unless otherwise stated. Statistical approaches for Table 1, Table S1 and Figure S9E have been described under *CYP27A1 IHC Analysis.*

Supplemental Text

Evaluation of the *in vitro* pharmacology of 27-hydroxycholesterol in cellular models of breast cancer.

A microarray analysis of mRNA expression was performed to compare the activities of 27-hydroxycholesterol (27HC) and 17-β-estradiol (E2) in MCF7 human breast cancer cells (fig. S1A) (*17*). The data from the E2 arm of this study have been published (GSE35428) but are included here for comparative purposes (*28*). Gene ontology analysis of the most robustly regulated genes (cutoff: $p<0.01$) revealed a role for 27HC in the regulation of cholesterol homeostasis, tamoxifen resistance and inflammatory IFN responses (fig. S1B). There was significant overlap between the genes identified and those previously shown to be regulated by the LXR agonist GW3965 in dendritic cells (GSE23073) (fig. S1C) (*33*). Follow-up studies revealed that 27HC regulated both ERα and LXR transcriptional activity in multiple ERα+ breast cancer cell lines (fig. S2A). Induction of the expression of the LXR responsive gene ABCA1 by 27HC, or synthetic LXR agonists, was increased upon inhibition of ERα by the antagonist ICI 182,780, or by ERα knockdown. Inhibition of LXRα/β enhanced 27HC mediated induction of ER target gene expression (fig. S2B, C). Increased proliferation was also observed in both 27HC or E2 treated MCF7 cells; an activity that was ablated upon ERα knockdown or co-treatment with the ER antagonist ICI 182,780 (fig. S2D). Interestingly, the mitogenic activity of E2 was inhibited by cotreatment with a pure LXR agonist and conversely the ER-dependent effects of 27HC on proliferation were accentuated following siRNA mediated knockdown or antagonist mediated inhibition of LXRα and β activity (fig. S2D). The same treatments had no effect in the ERα negative SKBR3 and MDA-MB-231 cell lines. Similarly the proliferation of these ERα-negative cell lines was unaffected by inhibitors of 27HC synthesis (CYP27A1 inhibitors), LXR antagonists or by LXR knockdown (fig. S3). Together these data highlight the complex interactions between ER and LXR and implicate these receptors as mediators of 27HC action in cellular models of breast cancer.

Fig. S1

27-hydroxycholesterol is a SERM and an LXR agonist. (A) Analysis of mRNA expression in MCF7 breast cancer cells indicates that 27HC induces the expression of genes generally associated with the activation of ER and LXR. (B) Heat map of genes with largest difference in regulation between 27HC and E2, with associated pathway analysis. (C) Cluster 2 genes from (B) have significant overlap with LXR target genes as identified in dendritic cells.

A

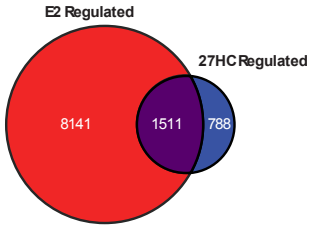
E2 Regulated
27HC Regulated
8141
1511
788

B

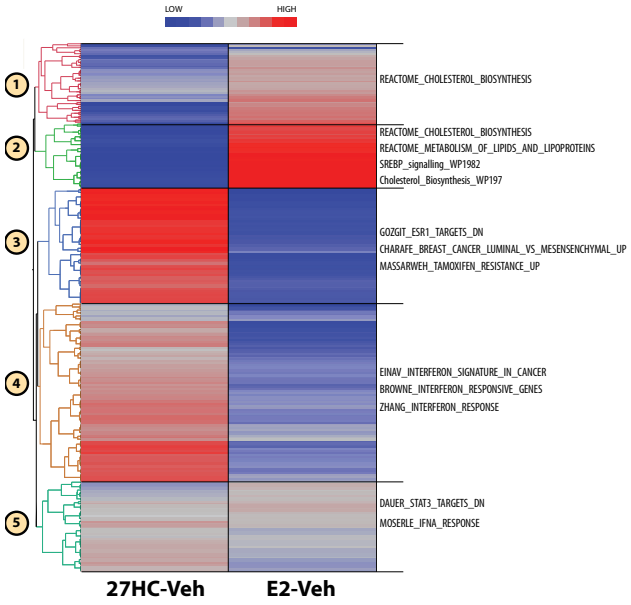
LOW
HIGH
1
2
3
4
5
REACTOME_CHOLESTEROL_BIOSYNTHESIS
REACTOME_CHOLESTEROL_BIOSYNTHESIS
REACTOME_METABOLISM_OF_LIPIDS_AND_LIPOPROTEINS
SREBP_signalling_WP1982
Cholesterol_Biosynthesis_WP197
GOZGIT_ESR1_TARGETS_DN
CHARAFE_BREAST_CANCER_LUMINAL_VS_MESENSENCHYMAL_UP
MASSARWEH_TAMOXIFEN_RESISTANCE_UP
EINAV_INTERFERON_SIGNATURE_IN_CANCER
BROWNE_INTERFERON_RESPONSIVE_GENES
ZHANG_INTERFERON_RESPONSE
DAUER_STAT3_TARGETS_DN
MOSERLE_IFNA_RESPONSE
27HC-Veh
E2-Veh

C

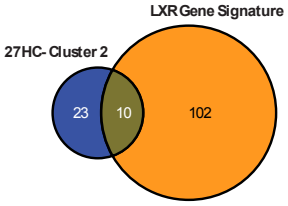
LXR Gene Signature
27HC- Cluster 2
23
10
102

Fig. S2

27-hydroxycholesterol is a modulator of both ER and LXR target gene expression in cellular models of ERα+ breast cancer. (A) 27HC and synthetic LXR ligands T1317 and GW3965 induce the expression of ER target genes (i.e. PS2) and LXR target genes (i.e. ABCA) in MCF7, T47D, BT483 and BT474 cells. (B) Induction of ER target genes is ablated upon ERα knockdown (siERα) or when ER activity is inhibited using the antagonist ICI 182,780. The induction of LXR target genes is enhanced upon knockdown of ERα expression or upon the addition of the ER antagonist ICI 182,780. (C) The effect of 27HC on LXR target genes is attenuated while its effect on ER target genes is enhanced in the absence of the LXRs (siLXRα/β) or when LXR activity is blocked with the antagonist GSK2033A. (D) 27HC induces MCF7 proliferation via the ER while its activation of LXRs decreases this effect. Different letters denote statistical significance (mean +/- SEM, $p<0.05$, $n \geq 3$).

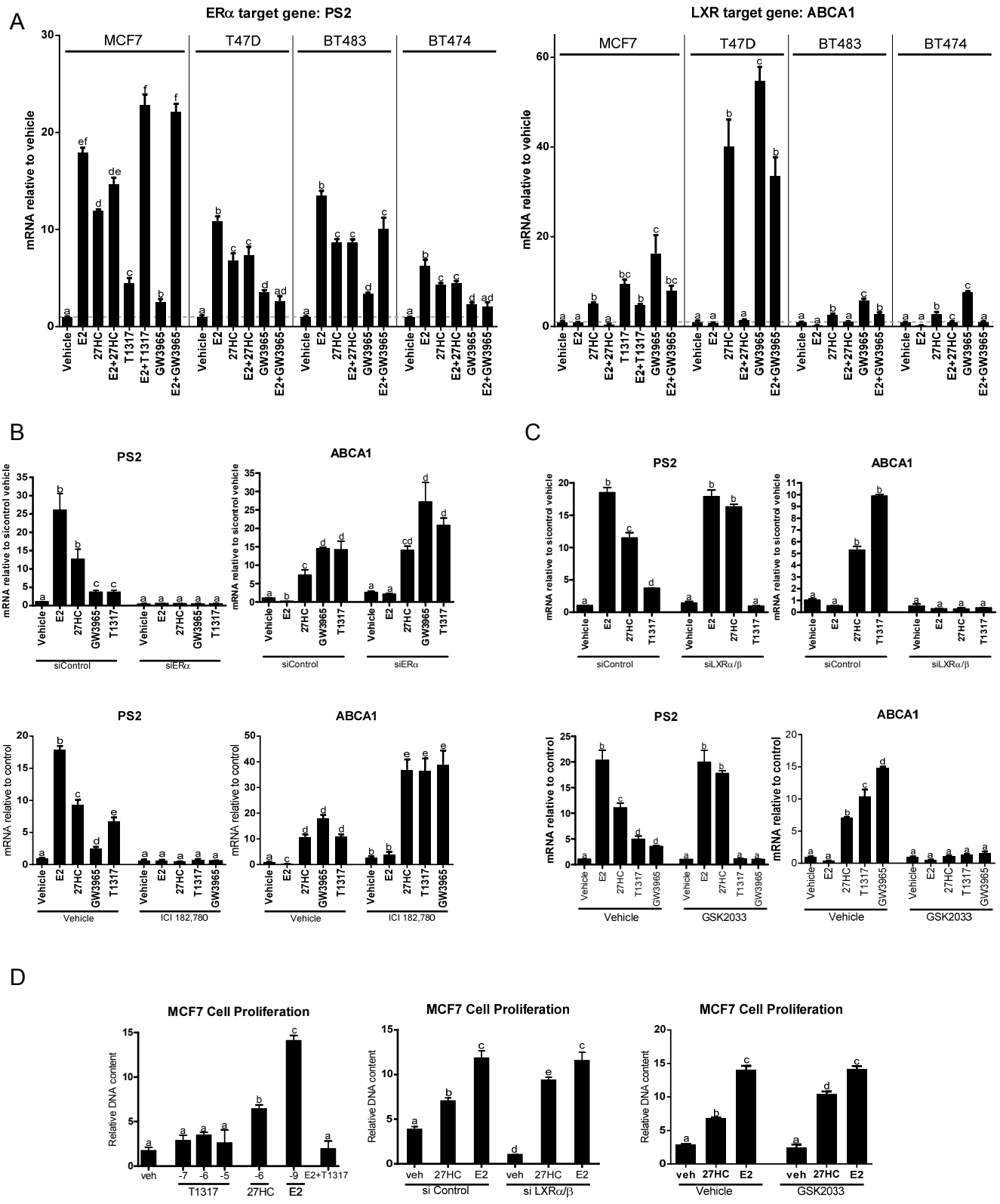
A
ERα target gene: PS2
LXR target gene: ABCA1
MCF7
T47D
BT483
BT474
mRNA relative to vehicle
Vehicle
E2
27HC
E2+27HC
T1317
E2+T1317
GW3965
E2+GW3965
B
PS2
ABCA1
mRNA relative to sicontrol vehicle
siControl
siERα
C
siLXRα/β
D
MCF7 Cell Proliferation
Relative DNA content
veh
T1317
27HC
E2
E2+T1317
si Control
si LXRα/β
Vehicle
GSK2033
ICI 182,780
mRNA relative to control

Fig. S3

27-hydroxycholesterol does not impact cell proliferation in the ER-negative cell lines, SKBR3 and MDA-MB-231. (A) Activation of LXRs by 27HC or synthetic LXR ligands does not alter cell proliferation. Time course and bar-graph representation of day 7 is indicated. The doses of 27HC, and the synthetic LXR ligands GW3965 and T0901317 (T1317) that were used for this study, are indicated (Log(M)). (B) Inhibition of CYP27A1 by the chemical inhibitors GW273297X (G297X) or GI268267X (G267X), or inhibition of LXRs by the antagonist GSK2033 or RNA interference does not alter proliferation. Bar-graph representation of day 7 is depicted. All data is presented as mean +/- SEM (n=3).

A

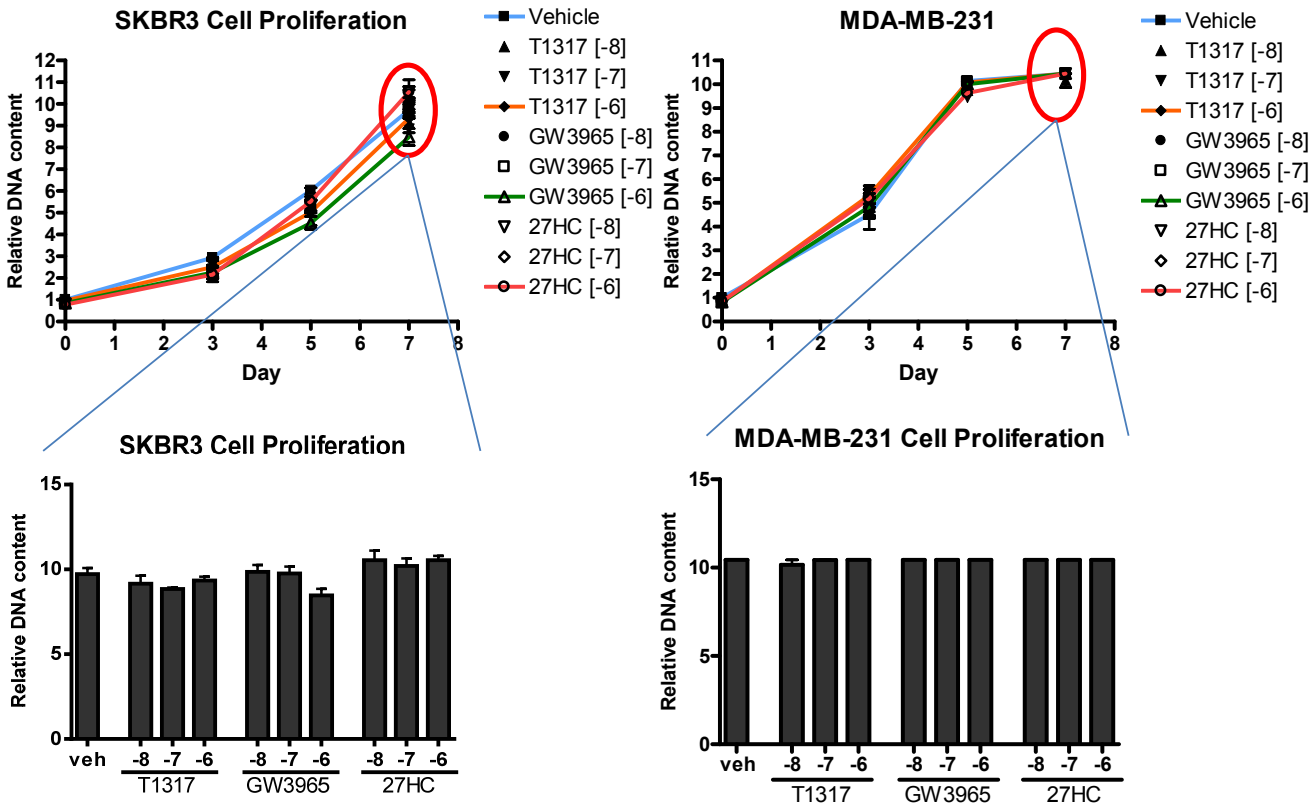
SKBR3 Cell Proliferation
Relative DNA content
Day
Vehicle
T1317 [-8]
T1317 [-7]
T1317 [-6]
GW3965 [-8]
GW3965 [-7]
GW3965 [-6]
27HC [-8]
27HC [-7]
27HC [-6]
MDA-MB-231
SKBR3 Cell Proliferation
MDA-MB-231 Cell Proliferation
veh
-8 -7 -6
T1317
GW3965
27HC

B

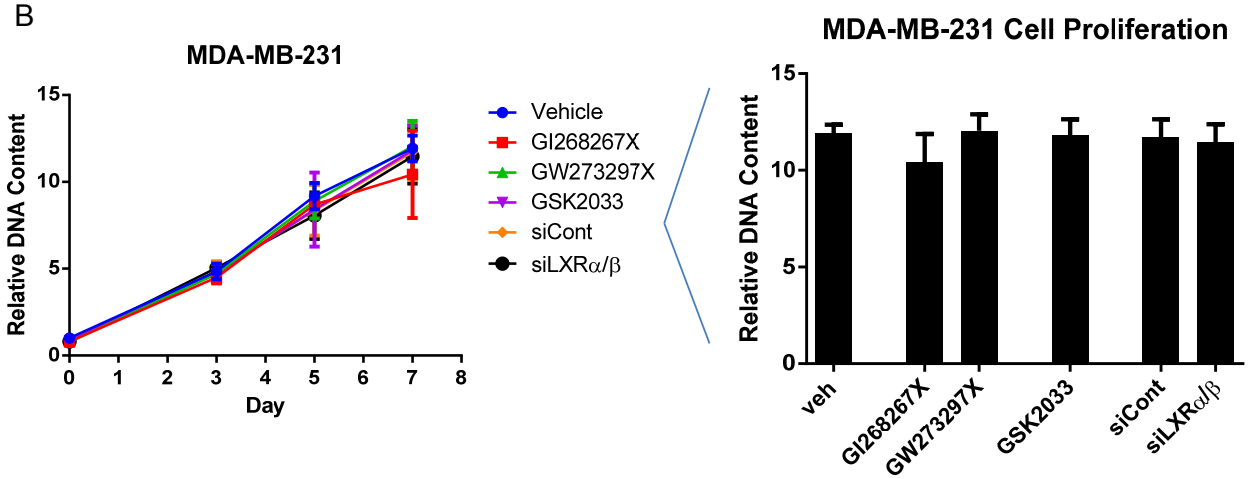
MDA-MB-231
Relative DNA Content
Day
Vehicle
GI268267X
GW273297X
GSK2033
siCont
siLXRα/β
MDA-MB-231 Cell Proliferation
veh
GI268267X
GW273297X
GSK2033
siCont
siLXRα/β

Fig. S4

MCF7 cell derived xenografts require supplementation with either 17-β-estradiol or 27-hydroxycholesterol for growth. Supplemental data to **Figure 1** indicating that when MCF7 cells are grafted into ovariectomized mice they do not grow unless mice are treated with either 17β-estradiol or 27HC. (mean +/- SEM, n = 5 for the no hormone group).

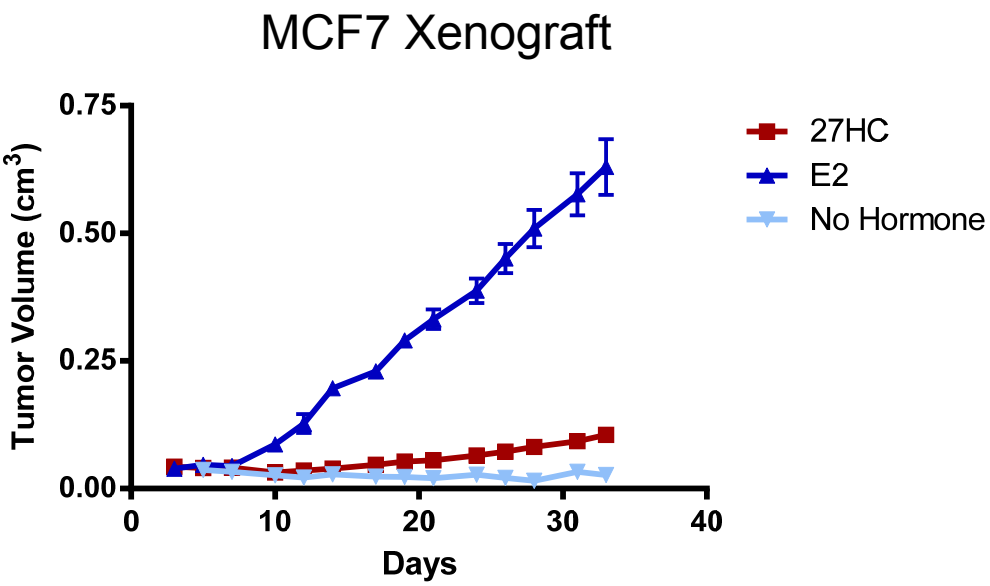
MCF7 Xenograft
Tumor Volume (cm3)
0.75
0.50
0.25
0.00
0
10
20
30
40
Days
27HC
E2
No Hormone

Fig. S5

Analysis of mRNA and protein expression in tumors from MMTV-PyMT mice treated with indicated ligands. (A) mRNA analysis of indicated genes by QPCR. Different letters denote statistical significance (mean +/- SEM, $p<0.05$, n = 6-18). (B) Micrographs depicting the proliferation marker Ki67. Scale bar = 200μm (C) Micrographs depicting the endothelial (angiogenesis) marker CD31. Scale bar = 200μm (D) Percentage of cells within tumor expressing the macrophage marker CD11b as determined by flow cytometry. Different letters denote statistical significance (mean +/- SEM, $p<0.05$, n = 4).

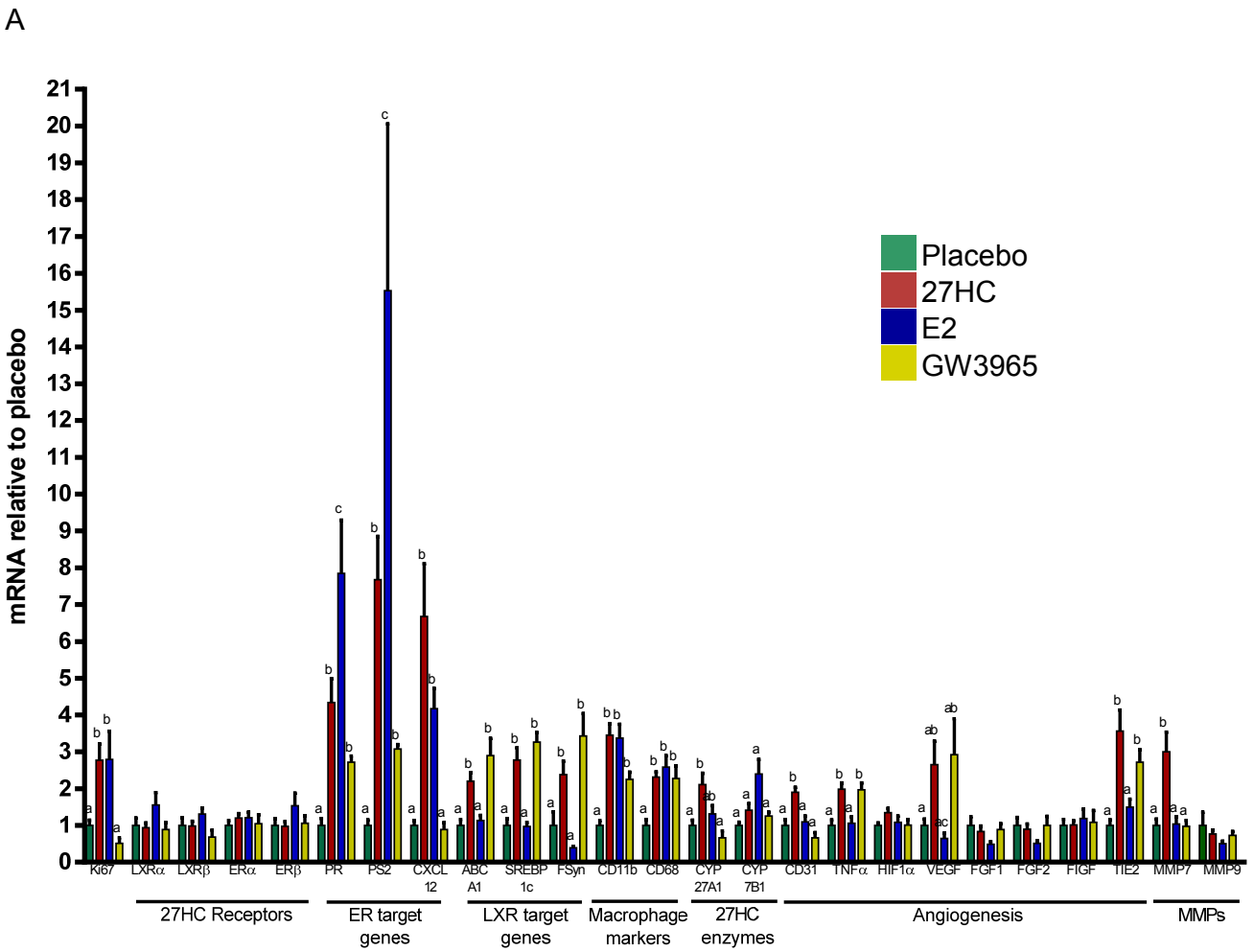
A
mRNA relative to placebo
Placebo
27HC
E2
GW3965
Ki67
LXRα
LXRβ
ERα
ERβ
PR
PS2
CXCL 12
ABC A1
SREBP 1c
FSyn
CD11b
CD68
CYP 27A1
CYP 7B1
CD31
TNFα
HIF1α
VEGF
FGF1
FGF2
FIGF
TIE2
MMP7
MMP9
27HC Receptors
ER target genes
LXR target genes
Macrophage markers
27HC enzymes
Angiogenesis
MMPs

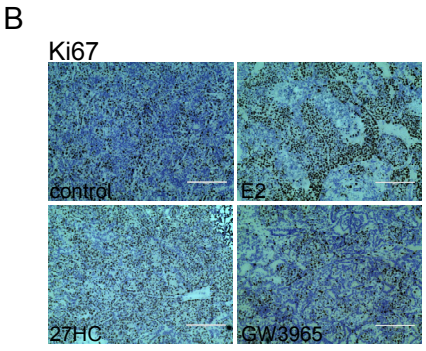
B
Ki67
control
E2
27HC
GW3965

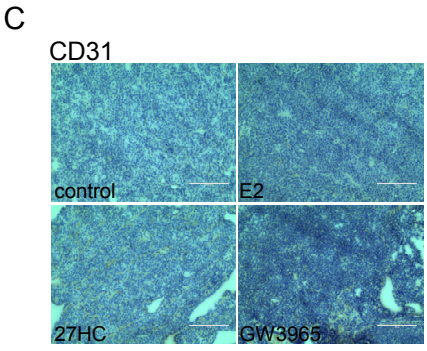
C
CD31
control
E2
27HC
GW3965

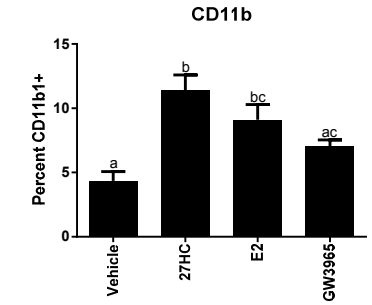
D
CD11b
Percent CD11b1+
Vehicle
27HC
E2
GW3965

Fig. S6

CYP7B1 mRNA expression tracks with a better prognosis in patients with luminal A type breast cancer while CYP27A1 mRNA expression is not associated with relapse free survival in patients classified with any subtype of breast cancer. (A) Relapse free survival curve based on CYP7B1 expression in patients classified with Luminal A type breast cancer (n = 1170). (B) Relapse free survival curves based on CYP27A1expression in patients classified with any type of breast cancer or only those diagnosed with Luminal A type (n = 1372 or 482 respectively).

A

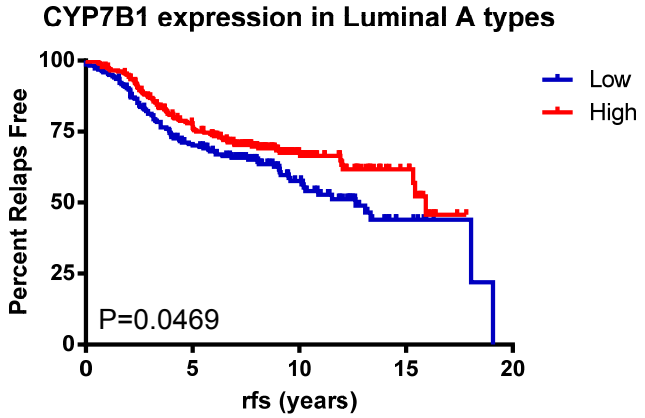
CYP7B1 expression in Luminal A types
Low
High
Percent Relaps Free
100
75
50
25
0
P=0.0469
0
5
10
15
20
rfs (years)

B

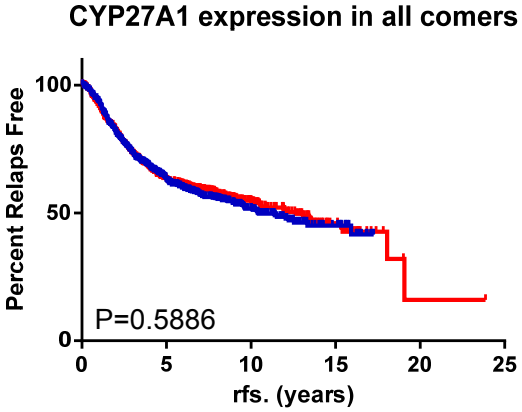
CYP27A1 expression in all comers
Percent Relaps Free
100
50
0
P=0.5886
0
5
10
15
20
25
rfs. (years)

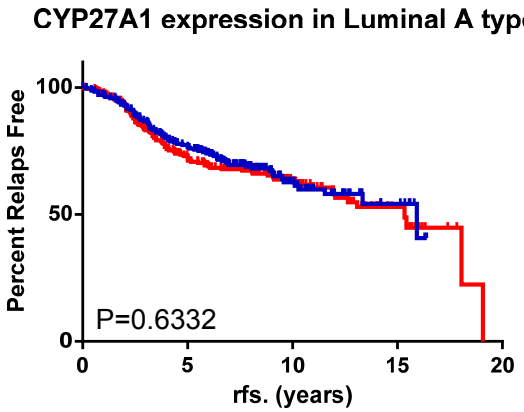
CYP27A1 expression in Luminal A types
Percent Relaps Free
100
50
0
P=0.6332
0
5
10
15
20
rfs. (years)

Fig. S7

The p450 oxidase CYP27A1 is highly expressed in macrophages within human benign and malignant mammary tissue. (A) Benign tissue depicting large duct with negatively staining epithelial lining and macrophages in lumen. (B) Benign tissue depicting weakly staining epithelium and strongly staining single stromal macrophage in center. (C) Negatively staining tumor nests with aggregate of strongly positive macrophages in stroma. (D) Negatively staining intraductal carcinoma with strongly positive macrophages in the lumen. A and C taken at 100x, scale bar = 40μm B and D taken at 400x, scale bar = 10μm.

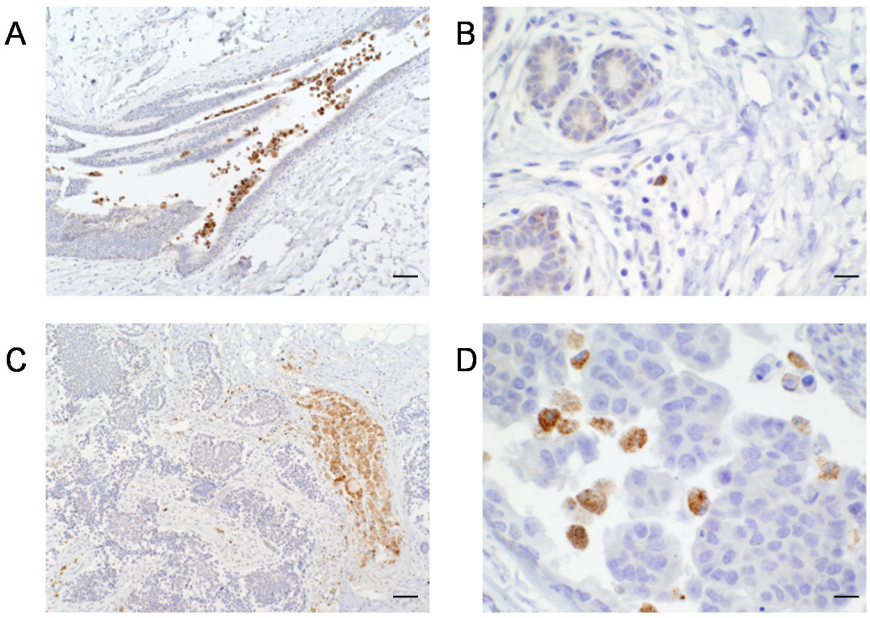
A
B
C
D

Fig. S8

Conditioned media from macrophages stimulates MCF7 cell proliferation.
Conditioned media was harvested from primary bone marrow derived macrophages that had been treated with the CYP27A1 inhibitors (A) GI268267X (G267X) or (B) GW273297X (G297X), or from (C) CYP27A1 null macrophages. Values at day 9 are indicated in bar graph format. (D) Conditioned media from macrophages induced the expression of ER target genes such as PS2 when added to MCF-7 cells. Different letters denote statistical significance (mean +/- SEM, $p<0.05$, n = 3-4). ICI = ICI 182,780

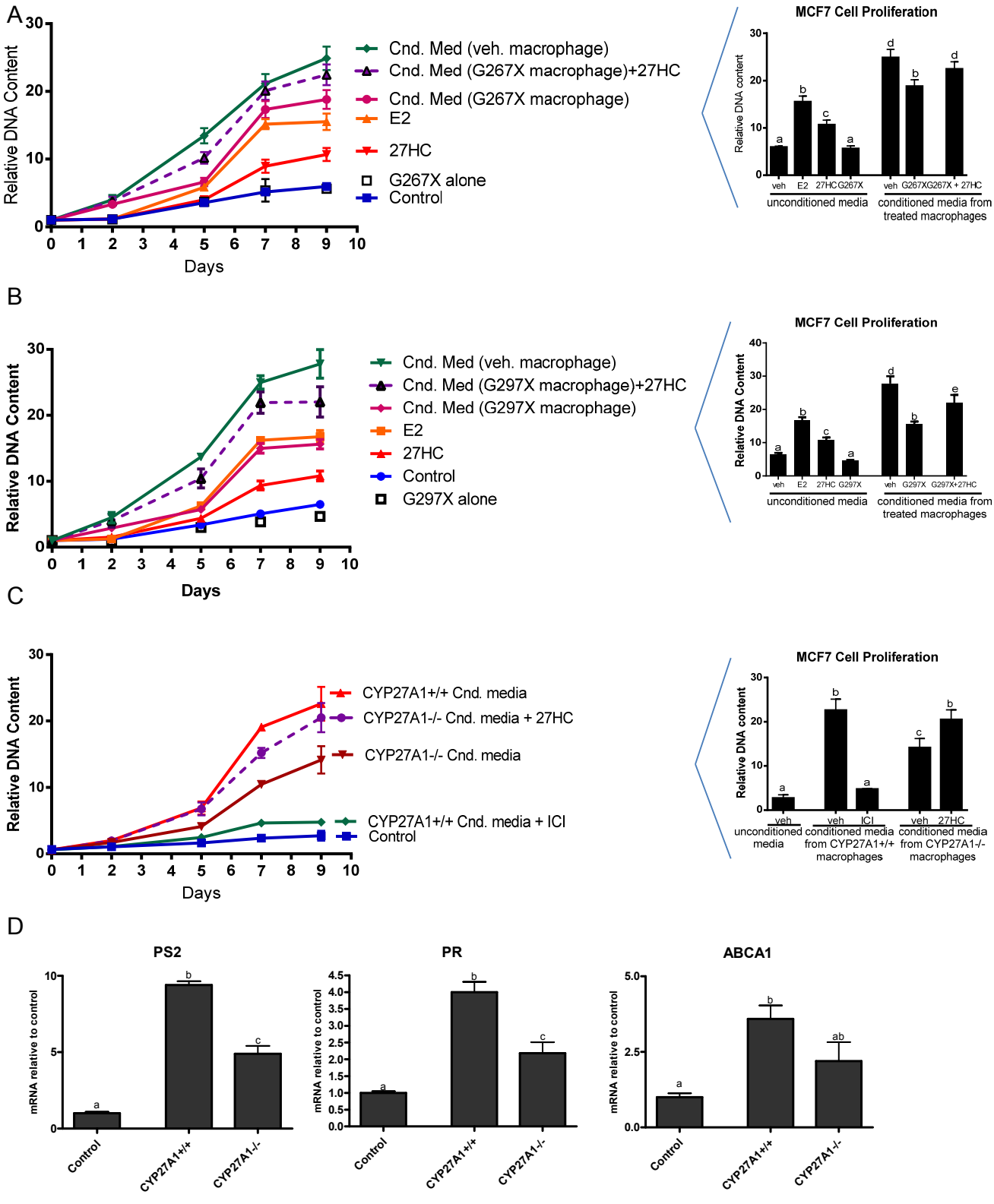
A
Relative DNA Content
Days
Cnd. Med (veh. macrophage)
Cnd. Med (G267X macrophage)+27HC
Cnd. Med (G267X macrophage)
E2
27HC
G267X alone
Control
MCF7 Cell Proliferation
Relative DNA content
veh E2 27HC G267X
veh G267X G267X + 27HC
unconditioned media
conditioned media from treated macrophages
B
Relative DNA Content
Days
Cnd. Med (veh. macrophage)
Cnd. Med (G297X macrophage)+27HC
Cnd. Med (G297X macrophage)
E2
27HC
Control
G297X alone
MCF7 Cell Proliferation
Relative DNA Content
veh E2 27HC G297X
veh G297X G297X+27HC
unconditioned media
conditioned media from treated macrophages
C
Relative DNA Content
Days
CYP27A1+/+ Cnd. media
CYP27A1-/- Cnd. media + 27HC
CYP27A1-/- Cnd. media
CYP27A1+/+ Cnd. media + ICI
Control
MCF7 Cell Proliferation
Relative DNA content
veh
veh ICI
veh 27HC
unconditioned media
conditioned media from CYP27A1+/+ macrophages
conditioned media from CYP27A1-/- macrophages
D
PS2
PR
ABCA1
mRNA relative to control
Control
CYP27A1+/+
CYP27A1-/-

Fig. S9

Breast cancer cell intrinsic expression of CYP27A1 protein is associated with tumor grade. Supplemental data for Table 1. Representative breast cancer TMA cores demonstrate a wide range of CYP27A1 expression within cancer cells. (A) negative staining, score = 0. (B) weak staining, score = 1. (C) moderate staining, score = 2. (D) strong staining, score = 3. Scale bars = 80μm. (E) Plot of probabilities indicating that an increase in CYP27A1 score from weak to overexpressed is associated with an increased probability of being grade 3 and a decreased probability of being a lower grade (1 or 2) (estimated odds ratio of 6.7 with interval of 1.7-26.6, p=0.007).

A

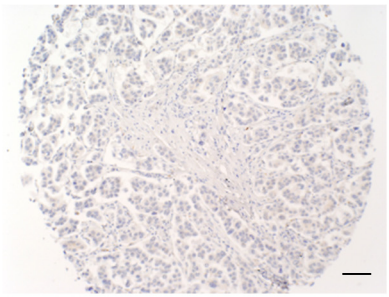

B

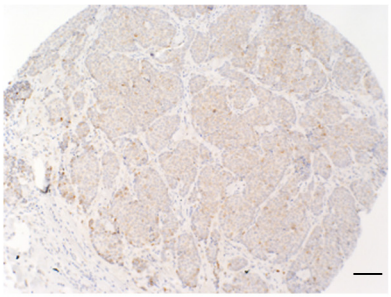

C

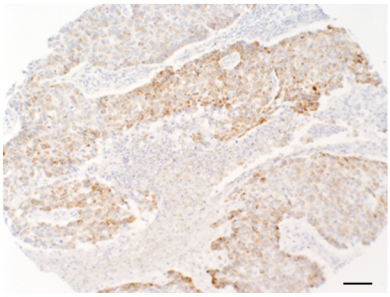

D

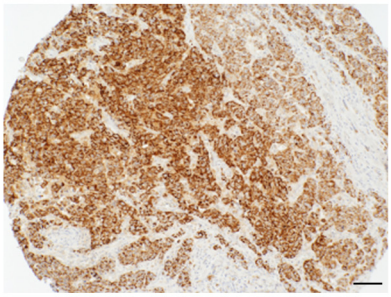

E

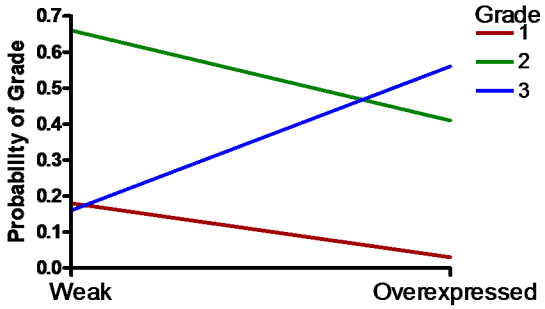
Probability of Grade
0.7
0.6
0.5
0.4
0.3
0.2
0.1
0.0
Weak
Overexpressed
Grade
1
2
3

Fig. S10

Cholesterol and 27hydroxycholesterol levels in in MMTV-PyMT mice fed a high cholesterol diet (HCD). Supplemental data to Figure 2A and B in text. (A) Plasma cholesterol levels (n = 7-9). (B) Intratumoral concentrations of 27HC. Values are ng of 27HC per g of wet tissue. (n = 3-6). ND = not detected. Statistics for (B) did not include $CYP27A1^{-/-}$ groups as no 27HC was detected. Values are mean +/- SEM and different letters denote statistical significance.

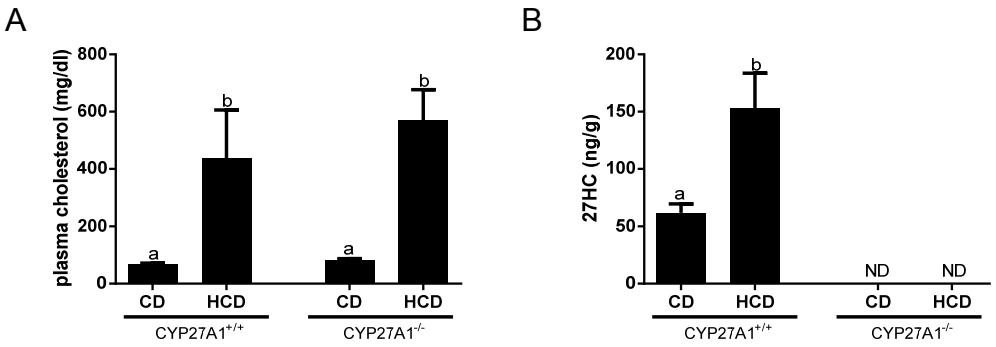
A
plasma cholesterol (mg/dl)
800
600
400
200
0
a
b
a
b
CD
HCD
CD
HCD
CYP27A1+/+
CYP27A1-/-
B
27HC (ng/g)
200
150
100
50
0
a
b
ND
ND
CD
HCD
CD
HCD
CYP27A1+/+
CYP27A1-/-

Fig. S11

The CYP27A1 inhibitor GW273297X decreases plasma and intratumoral 27hydroxycholesterol concentrations. Supporting data for Figure 2C. (A) A high fat diet (HFD) significantly increases total plasma cholesterol in *APOE3* mice compared to a control diet (CD) (n = 3-9). (B) Daily treatment of *APOE3* mice on a HFD with the CYP27A1 inhibitor GW273297X (GW297X) decreases plasma 27HC concentrations (mean +/- SEM, n = 3-4). (C) Intratumoral concentration of 27HC is decreased upon treatment with GW273297X in E0771 tumor bearing *APOE3* mice. Values are ng of 27HC per g of wet tissue (mean +/- SEM, n = 4). Different letters denote statistical significance ($p<0.05$).

A

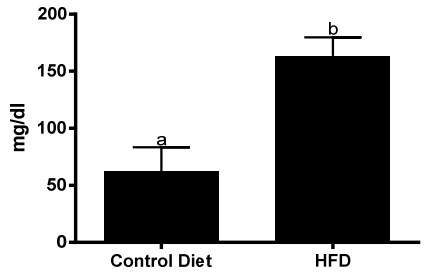
200
150
100
50
0
mg/dl
a
b
Control Diet
HFD

B

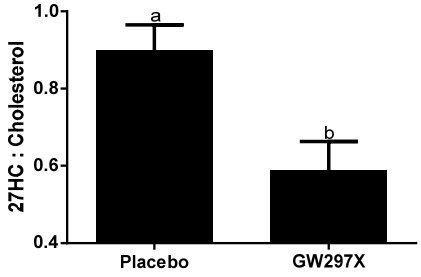
1.0
0.8
0.6
0.4
27HC : Cholesterol
a
b
Placebo
GW297X

C

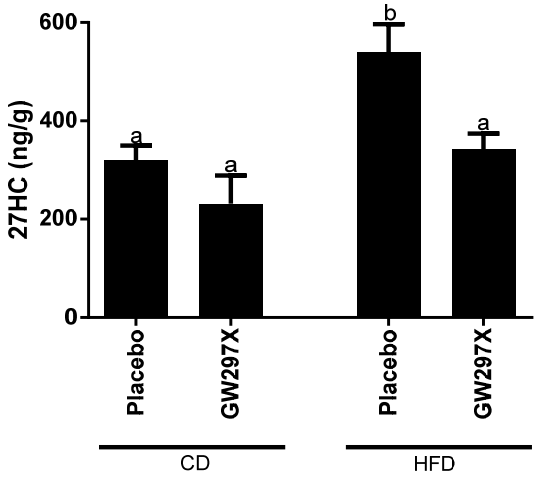
600
400
200
0
27HC (ng/g)
a
a
b
a
Placebo
GW297X
Placebo
GW297X
CD
HFD

Fig. S12

Statin treatment decreases total cholesterol and inhibits obesity driven tumor growth in the E0771 model of breast cancer. Supporting data for Figure 2D. (A) *apoE3* mice gain significant weight when fed a high fat diet (HFD) compared to a control diet (CD) for eight weeks (mean +/- SEM, n = 15/group). (B) Oral administration of atorvastatin (statin) from time of tumor graft (E0771 cells) decreases total plasma cholesterol to levels observed in CD fed mice. Different letters denote statistical significance (mean +/- SEM, n = 3-9). (C) There are linear relationships between obesity (% weight change) and final tumor volume, obesity and total plasma cholesterol, and total plasma cholesterol and final tumor volume. p-values indicate difference probability that the slope $\neq 0$.

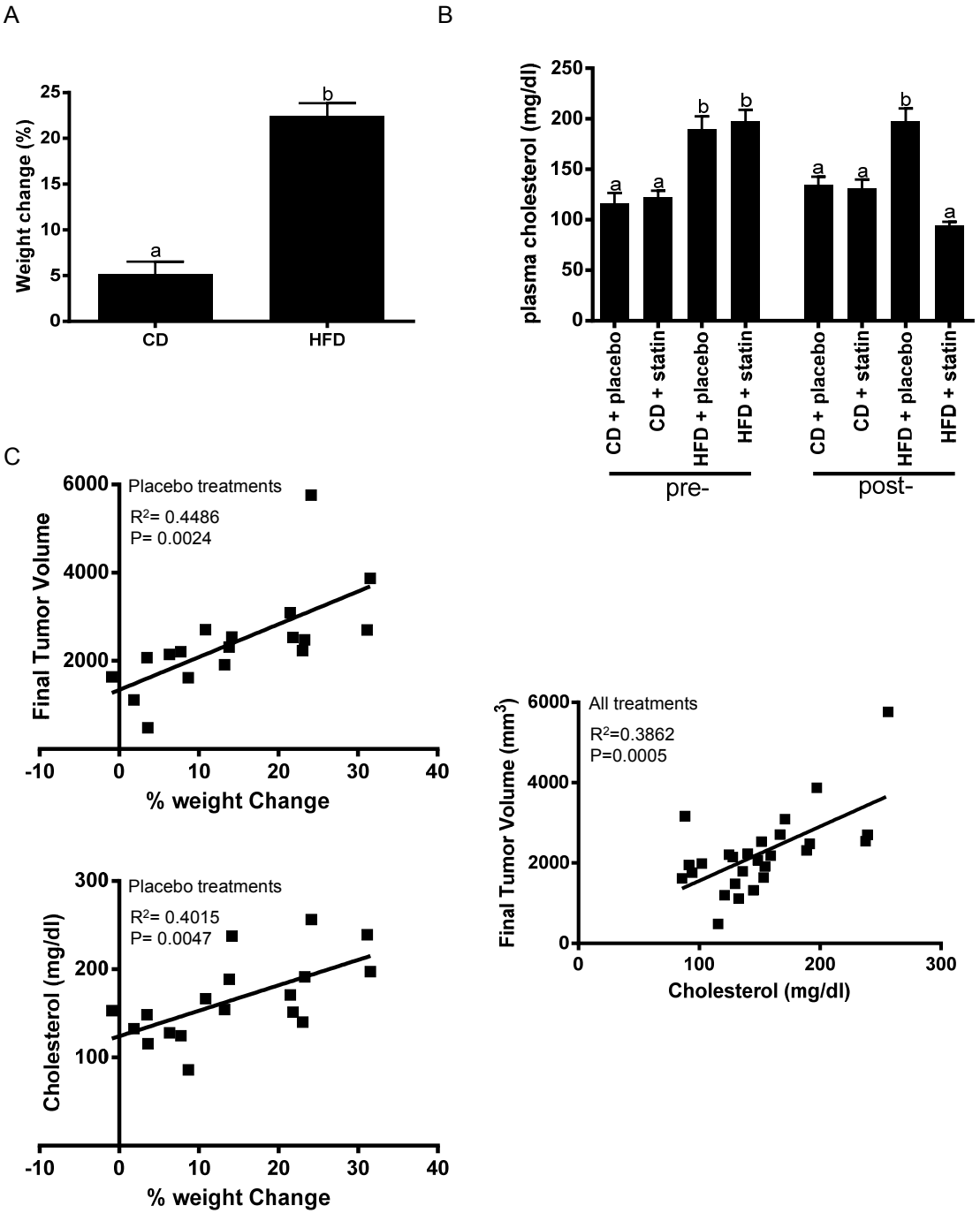
A
Weight change (%)
25
20
15
10
5
0
a
b
CD
HFD
B
plasma cholesterol (mg/dl)
250
200
150
100
50
0
a
a
b
b
a
a
b
a
CD + placebo
CD + statin
HFD + placebo
HFD + statin
CD + placebo
CD + statin
HFD + placebo
HFD + statin
pre-
post-
C
Final Tumor Volume
6000
4000
2000
Placebo treatments
R²= 0.4486
P= 0.0024
-10
0
10
20
30
40
% weight Change
Cholesterol (mg/dl)
300
200
100
Placebo treatments
R²= 0.4015
P= 0.0047
-10
0
10
20
30
40
% weight Change
Final Tumor Volume (mm³)
6000
4000
2000
All treatments
R²=0.3862
P=0.0005
0
100
200
300
Cholesterol (mg/dl)

Fig. S13

A high fat diet fails to impact tumor growth in the MMTV-PyMT mouse model of mammary cancer. High fat diet does not result in increased circulating cholesterol in the FVB strain of mice used for these studies and has no impact on tumor growth or latency. (A) PyMT Mice fed a high fat diet (HFD) fed from weaning are heavier compared to a control diet (CD) fed mice. Different letters denote statistical significance (mouse age 65-75d, mean +/- SEM, n=7-8, $p<0.05$). (B) HFD fails to significantly alter total plasma cholesterol in this mouse strain (mean +/- SEM, n=4-8). (C) Tumor latency was determined by age at which a palpable tumor was detected. (D) Once a palpable tumor formed, its size was measured and plotted as time to reaching a size of $1000mm^3$. (n = 14-15).

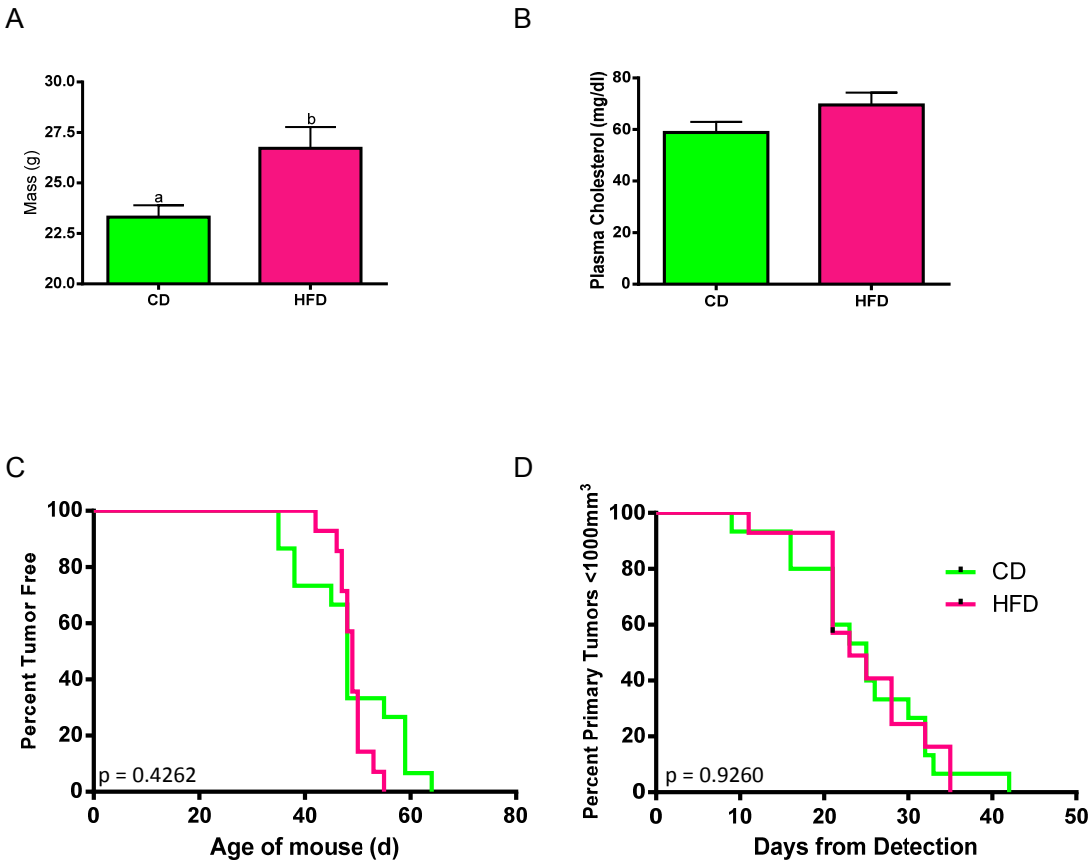
A
B
30.0
27.5
25.0
22.5
20.0
Mass (g)
a
b
CD
HFD
80
60
40
20
0
Plasma Cholesterol (mg/dl)
CD
HFD
C
D
100
80
60
40
20
0
Percent Tumor Free
p = 0.4262
0
20
40
60
80
Age of mouse (d)
Percent Primary Tumors <1000mm3
p = 0.9260
CD
HFD
0
10
20
30
40
50
Days from Detection

Fig. S14

27-hydroxcholesterol and the LXR agonist GW3965 modulate the expression of genes associated with EMT. (A) 27HC and GW3965 modulate mRNA expression of genes associated with EMT. c: control, 2: 27HC, G:GW3965. (B) 27HC and GW3965 induce Snail1 expression. Overlaid images of green (Snail1) and blue (dapi nuclear stain). (C) 27HC and GW3965 induce FAPα (separase) expression. Overlaid images of green (FAPα) and blue (dapi nuclear stain). All images were adjusted to 90% brightness and 100% contrast. Scale bar = 200μm.

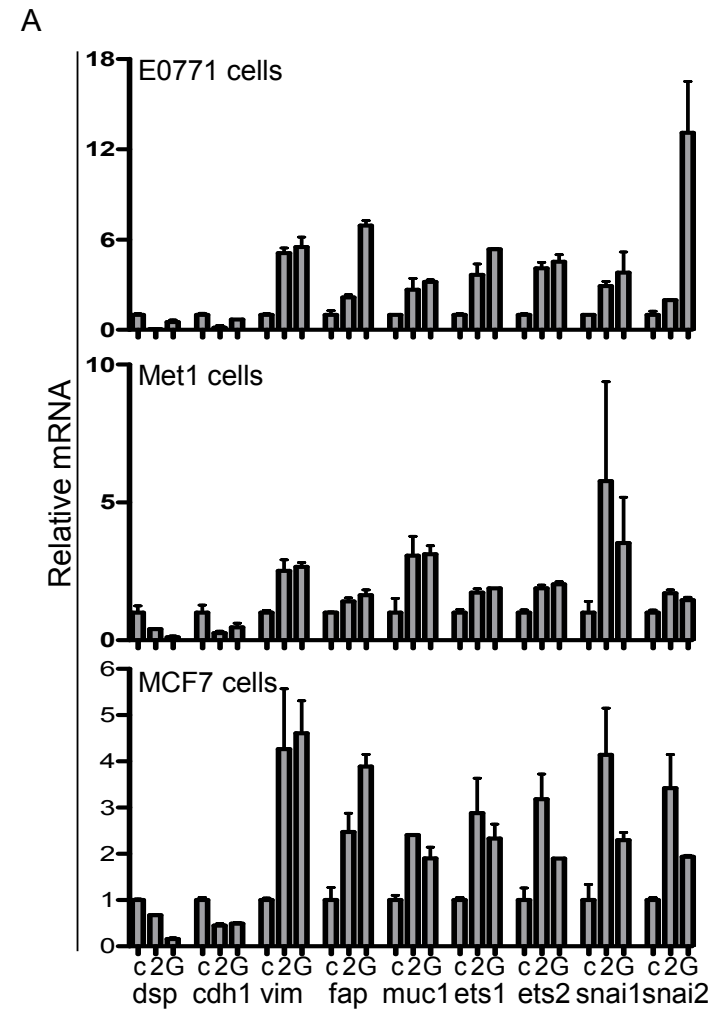
A
E0771 cells
Met1 cells
MCF7 cells
Relative mRNA
18
12
6
0
10
5
0
6
5
4
3
2
1
0
c 2G
dsp
cdh1
vim
fap
muc1
ets1
ets2
snai1
snai2

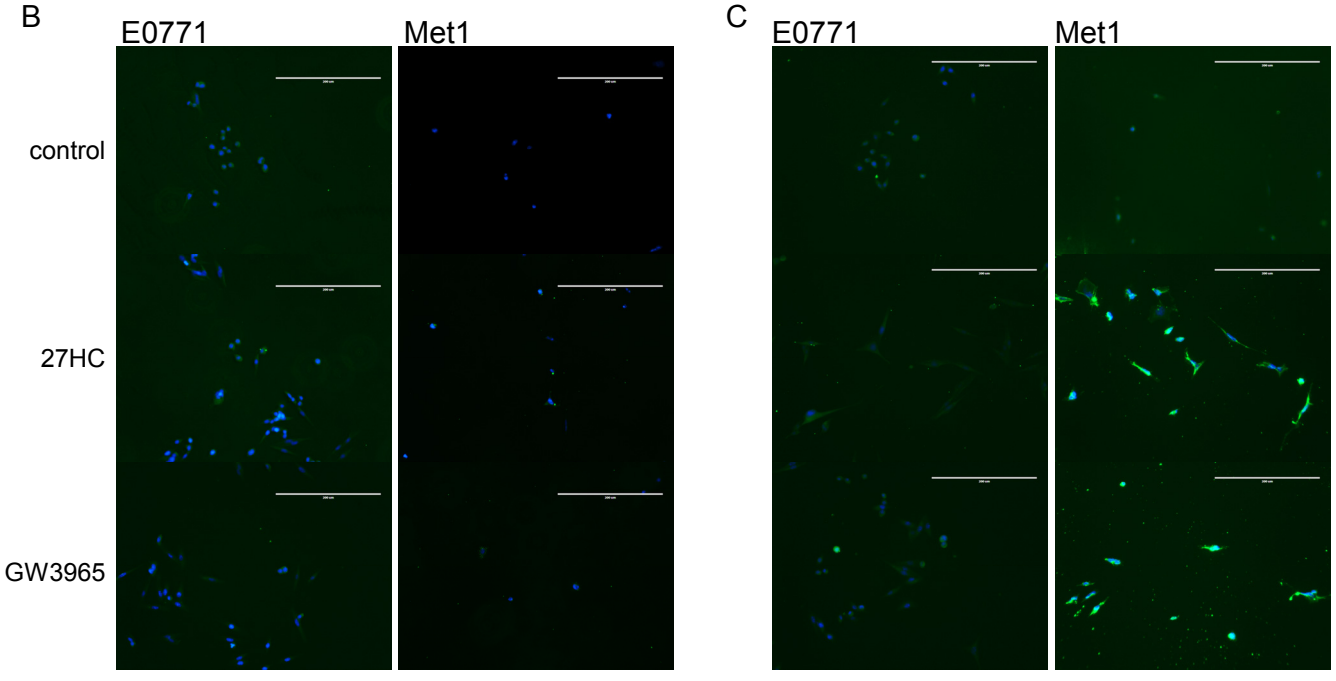
B
E0771
Met1
control
27HC
GW3965
C
E0771
Met1